

Effects of Heat Treatments on the Properties of Copper Phthalocyanine Films Deposited by Glow-Discharge-Induced Sublimation

Gianluigi Maggioni,^{*,†,‡,§} Sara Carturan,^{†,‡} Michele Tonezzer,^{†,§} Marco Bonafini,[†] Alberto Vomiero,^{†,||} Alberto Quaranta,[§] Chiara Maurizio,[⊥] Francesco Giannici,[#] Antonino Scandurra,[●] Francesco D'Acapito,[⊥] Gianantonio Della Mea,^{†,§} and Orazio Puglisi[○]

Istituto Nazionale di Fisica Nucleare, Laboratori Nazionali di Legnaro, Viale dell'Università 2, 35020 Legnaro, Padova, Italy

Received February 7, 2006. Revised Manuscript Received May 22, 2006

Copper phthalocyanine films have been deposited by glow-discharge-induced sublimation. The films have undergone postdeposition heat treatments in air at 250 and 290 °C for different times, ranging from 30 min to 14 h. The properties of as-deposited and heated films have been investigated by different techniques in order to determine the effects of heat treatments on the film properties. Fourier transform infrared analysis and UV–visible optical absorption analysis point out a gradual evolution of the film structure from a mixture of α and β polymorphs to the only β polymorph in the sample heated at 290 °C for 14 h. A pronounced decrease of carbon and nitrogen atomic percentages against an oxygen increase in the heated films are shown by ion beam analyses (Rutherford backscattering spectrometry and nuclear reaction analysis) and X-ray photoelectron spectroscopy (XPS). X-ray absorption spectroscopy and XPS indicate that part of the copper phthalocyanine molecules decompose during heat treatments and the formation of copper oxide takes place. The replacement of copper phthalocyanine by copper oxide in the heated films accounts for the change of their surface electrical conductance and of their electrical response to NO₂.

1. Introduction

Metal phthalocyanines (MPcs) are organic semiconductors which have attracted a great deal of interest for many years due to their peculiar properties such as thermal and chemical stability, photoconductivity, vacuum compatibility, and biocompatibility. MPcs films have found important applications in many different fields, including chemical sensing,¹ photoconducting agents,² photovoltaic cell elements for energy generation,³ nonlinear optics,⁴ and electrocatalysis.⁵ In the gas sensing field, MPcs films have been widely studied as electrical gas sensors:⁶ the sensing mechanism is based on the conductivity changes induced by the adsorption of oxidizing or reducing gases. Low concentrations of gases

such as NO_x, halogens, NH₃, and H₂O^{1,6} have been measured using conductivity-based devices but the transformation of the tested devices to real sensors is still lacking.

MPcs-based electrical gas sensors can operate at temperatures as low as 100 °C⁷ and even 30 °C,⁸ but in order to improve sensitivity and reversibility of the sensor response, these devices usually work at temperatures equal to or higher than 150 °C.⁹ However, the working temperature cannot be arbitrarily increased since the higher the temperature, the shorter the sensor lifetime.¹⁰ Moreover, Lee et al.¹¹ showed that evaporated copper phthalocyanine (CuPc) films operating at 225 °C under NO₂ atmosphere undergo a structure transformation which degrades the sensing characteristics. To obtain short response and recovery times, MPcs films have also been preheated at temperatures of 250–340 °C,^{12–14} but these treatments can give rise to a grain growth and to a more compact structure which decrease the electrical response to NO₂.¹¹ Taking into account all these aspects, the

* To whom correspondence should be addressed. E-mail: maggioni@lnl.infn.it.

† Istituto Nazionale di Fisica Nucleare.

‡ University of Padua.

§ Department of Materials Engineering and Industrial Technologies, University of Trento.

|| Presently at CNR-INFM SENSOR Lab, Via Valotti 9, 25133 Brescia, Italy.

⊥ CNR-INFM c/o European Synchrotron Radiation Facility GILDA-CRG, Grenoble, France.

Department of Inorganic and Analytical Chemistry, University of Palermo.

● Laboratorio Superfici e Interfasi – Consorzio Catania Ricerche.

○ Dipartimento di Scienze Chimiche, University of Catania.

- (1) Snow, A. W.; Barger, W. R. *Phthalocyanines: properties and applications*; Leznoff, C. C., Lever, A. B. P., Eds.; VCH Publishers: New York, 1989; Vol. 1, p 341.
- (2) Law, K.-Y. *Chem. Rev.* **1993**, *93*, 449.
- (3) (a) Wöhrle, D.; Kreienhoop, L.; Schlettwein, D. *Phthalocyanines: properties and applications*; Leznoff, C. C., Lever, A. B. P., Eds.; VCH Publishers: New York, 1996; Vol. 4, p 219. (b) Anthopoulos, T. D.; Shafai, T. S. *Thin Solid Films* **2003**, *441*, 207.
- (4) de la Torre, G.; Vazquez, P.; Agullo-Lopez, F.; Torres, T. *J. Mater. Chem.* **1998**, *8*, 1671.
- (5) Böttger, B.; Schindewolf, U.; Avila, J. L.; Rodriguez-Amaro, R. *J. Electroanal. Chem.* **1997**, *432*, 139.

(6) Guillaud, G.; Simon, J.; Germain, J. P. *Coord. Chem. Rev.* **1998**, *178–180*, 1433.

(7) Zhou, Q.; Gould, R. D. *Thin Solid Films* **1998**, *317*, 436.

(8) Newton, M. I.; Starke, T. K. H.; Willis, M. R.; McHale, G. *Sens. Actuators B* **2000**, *67*, 307.

(9) Lee, Y. L.; Hsiao, C. H.; Chang, C. H.; Yang, Y. M. *Sens. Actuators B* **2003**, *94*, 169.

(10) Mrwa, A.; Friedrich, M.; Hofmann, A.; Zahn, D. R. T. *Sens. Actuators B* **1995**, *24–25*, 596.

(11) Lee, Y. L.; Hsiao, C. Y.; Hsiao, R. H. *Thin Solid Films* **2004**, *468*, 280.

(12) Jones, T. A.; Bott, B.; Thorpe, S. C. *Sens. Actuators* **1989**, *17*, 467.

(13) Sadaoka, Y.; Jones, T. A.; Gopel, W. *Sens. Actuators B* **1990**, *1*, 148.

(14) Liu, C. J.; Hsieh, J. C.; Ju, Y. H. *J. Vacuum Sci. Technol. A* **1996**, *14*, 753.

study of the effects of heat treatments on the properties of MPCs films is then particularly important for the final application of these materials since commercial sensing devices must be working for months or years without significant changes of their performances.

In a previous work the effects of heat treatments on the physical properties of CuPc films deposited by glow-discharge-induced sublimation (GDS) were investigated by using X-ray diffraction (XRD), Fourier transform infrared analysis (FT-IR), scanning electron microscopy (SEM), and UV-Visible absorption analysis.¹⁵ It was found that heat treatments at 250 and 290 °C for 14 h in air strongly changed the structure and morphology of GDS films. In particular, the structural disorder of the as-deposited films decreased after the treatment at 250 °C and the complete disappearance of the α -phase after 14 h at 290 °C took place.

The aim of the present work is to study in more detail the effects of the heat treatments on GDS films using specific techniques such as ion beam analysis (IBA), extended X-ray absorption fine structure spectroscopy (EXAFS), X-ray absorption near edge structure spectroscopy (XANES), and X-ray photoelectron spectrometry (XPS). Ion beam analysis allows measurement of the changes of the elemental film composition induced by heat treatments. On the other hand, X-ray absorption spectroscopies (XAS) are elective tools to investigate the local structure around Cu atoms in the CuPc films¹⁶ because they can give information on the very first shell of atoms surrounding a selected atomic species,^{17,18} Cu in this case. In particular, the EXAFS spectroscopy has been used to characterize the first shell of atoms around Cu, in terms of coordination number and average shell radius. Information has been obtained on the Cu oxidation state in as-deposited and heated CuPc films by XANES spectroscopy and XPS analysis.

To follow the evolution of the physical changes at increasing heating time, the GDS films have been heated at 290 °C for times ranging from 30 min to 4 h. The changes have been studied by FT-IR, IBA, SEM, and UV-visible absorption analysis. The effects on the surface electrical conductance have also been measured and related to the corresponding changes of the film composition during the heat treatments.

In view of the application of these films to gas-sensing measurements, the effects of heat treatments on the electrical response of GDS films to NO₂ have been tested by exposing the samples to a NO₂-containing gas mixture and measuring the resulting change of their electrical conductance.

2. Experimental Section

The experimental apparatus used for the deposition of CuPc films consisted of a vacuum chamber evacuated to a base pressure of 10⁻⁴ Pa. The glow discharge was sustained by a 1-in. cylindrical

magnetron sputtering source connected to a radio frequency power generator (600 W, 13.56 MHz) through a matching box. The CuPc powder (750 mg, 99.5% purity, Acros Organics) was put on the surface of an aluminum target, placed on the sputtering source. The glow discharge feed gas was argon (99.9999%). Typical values of rf power, target dc self-bias, and working pressure were in the ranges 10–20 W, –20 to –300 V, and 5.00 ± 0.05 Pa, respectively. The CuPc films were deposited on three different substrates: P-doped (100) silicon wafer 350- μ m thick lapped on both faces (Atomergic Chemetals Inc.) for IBA, FT-IR, and SEM measurements; quartz glass slide (PGO GmbH) for UV-Vis analysis and electrical measurements; 25 μ m thick Kapton films (Goodfellow) for XAS and XPS. For the electrical measurements 23 gold parallel rectangular electrodes (0.68 mm far apart) were evaporated on the quartz slides before CuPc deposition. The substrates were mounted on a sample holder placed 7 cm above the source. To have a set of reliable reference samples for XAS measurements, CuPc films were also deposited onto Kapton substrates by vacuum evaporation (VE), which is most widely used for the deposition of MPC films. The vacuum evaporation apparatus has been described elsewhere.¹⁹ The thickness of evaporated and GDS-deposited films ranged from 1 to 2 μ m.

The GDS samples underwent heat treatments in air at 250 °C for 14 h and at 290 °C for times ranging from 30 min to 14 h, while the treatment time of the VE films was limited to 14 h for both temperatures.

The measurement of the film composition was performed by ion beam analyses at the Van de Graaff accelerators at the Laboratori Nazionali di Legnaro on CuPc coatings deposited on silicon substrates. Low-beam current density on the sample (about 1 μ A/cm²) was applied in order to accurately measure the ion fluence at the beginning of the spectrum collection and to reduce sample heating and damage during IBA. Copper concentration was determined by Rutherford backscattering spectrometry (RBS) using a 2.2 MeV ⁴He⁺ beam, at the scattering angle of 160°, whereas nitrogen, carbon, and oxygen concentrations were measured by nuclear reaction analysis (NRA) using a 0.83 MeV ²H⁺ beam. Since the organic materials can be heavily damaged during analysis and the desorption of volatile species from the sample surface leads to the invalidation of the experimental results, this process was monitored during spectra acquisition. No desorption of C, N, and O was revealed under ion bombardment during NRA.

FT-IR spectra of the samples were recorded in the 4000–400 cm⁻¹ range using a Jasco FT-IR 660 Plus spectrometer with a resolution of 4 cm⁻¹. The sample cell and the interferometer were evacuated in order to remove the absorption peaks of water and atmospheric gases.

The surface morphology of the samples was investigated by a scanning electron microscope (SEM, Philips XL-30).

A Jasco V-570 dual-beam spectrophotometer was used to perform the UV-visible absorption measurements in the 200–800 nm range, with a resolution of 2 nm.

XAS experiment was performed at the Cu K-edge (8979 eV) at the GILDA-CRG beamline²⁰ of the European Synchrotron Radiation Facility (ESRF) in Grenoble (France). The monochromator, working in dynamical focusing mode,²¹ was equipped with two Si 311

(15) Maggioni, G.; Quaranta, A.; Carturan, S.; Patelli, A.; Tonzeller, M.; Ceccato, R.; Della Mea, G. *Chem. Mater.* **2005**, *17*, 1895.

(16) Carrera, F.; Marcos, E. S.; Merkling, P. J.; Chaboy, J.; Munoz-Paez, A. *Inorg. Chem.* **2004**, *43*, 6674.

(17) *X-ray Absorption: principles and application techniques of EXAFS, SEXAFS and XANES*; Konigsberger, D. C., Prins, R., Eds.; J. Wiley & Sons: New York, 1988.

(18) Rehr, J. J.; Albers, R. C. *Rev. Mod. Phys.* **2000**, *72*, 621.

(19) Maggioni, G.; Carturan, S.; Boscarino, D.; Della Mea, G.; Pieri, U. *Mater. Lett.* **1997**, *32*, 147.

(20) D'Acapito, F.; Colonna, S.; Pascarelli, S.; Antonioli, G.; Balerna, A.; Bazzini, A.; Boscherini, F.; Campolungo, F.; Chini, C.; Dalba, G.; Davoli, G. I.; Fornasini, F.; Graziola, R.; Licheri, G.; Meneghini, C.; Rocca, F.; Sangiorgio, L.; Sciarra, V.; Tullio, V.; Mobilio, S. *ESRF Newsletter* **1998**, *30*, 42.

(21) Pascarelli, S.; Boscherini, F.; D'Acapito, F.; Hrdy, J.; Meneghini, C.; Mobilio, S. *J. Synchrotron Radiat.* **1996**, *3*, 147.

Table 1. Heat Treatments and Analyses Performed on the CuPc Samples^a

sample name	IBA	FT-IR	UV-V is	SEM	EXAFS-XANES	XPS	electrical conductivity	response to NO ₂
GDS Samples								
as-deposited	ASDEP	o	o	o	o	o	o	o
290 °C 30 min	290C30	o	o	o	o	o	o	o
290 °C 1 h	290C1h	o	o	o	o	o	o	o
290 °C 2 h	290C2h	o	o	o	o	o	o	o
290 °C 3 h	290C3h	o	o	o	o	o	o	o
290 °C 4 h	290C4h	o	o	o	o	o	o	o
290 °C 14 h	290C14h	o	o	o	/	o	o	o
250 °C 14 h	250C14h	o	/	/	/	o	o	o
Evaporated Samples								
as-deposited	EVASDEP	/	/	/	o	o	o	o
250 °C 14 h	EV250C14h	/	/	/	o	o	o	o
290 °C 14 h	EV290C14h	/	/	/	o	o	o	o

^a An asterisk indicates that the results of the corresponding analysis are reported in a previous work.¹⁵

crystals and the harmonics rejection was achieved by a couple of Pd-coated mirrors with an energy cutoff of 21 keV. All the samples were exposed to air just before the measure, and the X-ray absorption spectra were recorded at room temperature; due to sample dilution, XAS spectra were measured in fluorescence mode by a 13-element high-purity Ge detector. X-ray absorption spectra of a CuPc powder pellet and CuO crystalline powder were recorded as reference standards in transmission mode, while the X-ray absorption spectrum of a CuPc solution (in toluene, ca. 0.1 mM) was recorded in fluorescence mode. For the data analysis, the EXAFS spectra were obtained from the measured X-ray absorption spectrum by using Autobk program,²² minimizing the low-frequency part of the spectrum according to standard procedure. The obtained EXAFS signals were Fourier-transformed using a symmetrical Hanning window ranging from $k = 3-8 \text{ \AA}^{-1}$, and first shell fit was performed on all samples in the R -space by using Ifeffit software,²³ with theoretical amplitudes and phases calculated by the Feff8.2 code²⁴ for the Cu-N coordination of a complete CuPc molecule.²⁵ The S_0^2 parameter of the standard EXAFS formula,¹⁸ the energy edge shift, and the Debye-Waller factor σ^2 were obtained by fitting the CuPc standard spectrum and then used as fixed parameters for fitting the EXAFS spectra of the GDS samples. The uncertainties reported on the fitting results (see Table 3) correspond to a confidence level of 68%.

XPS analyses were performed using a Kratos AXIS-HS spectrometer equipped with Mg $K\alpha_{1,2}$ (1253.6 eV) X-ray source (10 mA, 15 keV). The instrumental transmission operates in fixed analyzer transmission (FAT) mode. A pass energy of 40 eV was selected which allows an intrinsic full-width at half-maximum (fwhm) of 0.8 eV. To deconvolute the various peak components, a Gaussian curve fitting procedure was made after linear background subtraction. Literature data^{26,27} were used as a reference for the assignment of the peak components. Quantitative data were obtained from the experimental peak area using a computer routine based on empirically derived atomic sensitivity factors.

Electrical measurements were performed with an electrometer (Keithley Instruments, model 237). Electrical surface conductance was measured on CuPc films deposited onto interdigitated gold electrodes on silica substrates. The CuPc samples were put inside

a measurement chamber equipped with two mass flow controllers (STEC E440J): the former allows control of the flow rate of NO₂-containing mixture between 1 and 1000 sccm; the latter controls the flow rate of pure nitrogen from 1 to 5000 sccm. A PC is connected to a ROD-2M control unit featuring two channels; each is connected in turn to a mass flow controller. This way it is possible to use the PC to simultaneously control both fluxes, greatly reducing the time delays. For the measurement of the surface conductance a background pressure of 10⁵ Pa of flowing N₂ (1000 sccm) was fixed. A ceramic heater was used to increase the sample temperature up to 170 °C. The surface conductance was measured at a fixed voltage (1 V) at increasing and decreasing temperature.

Electrical response to NO₂ was measured after heating the samples up to 150 °C under N₂ flow (500 sccm). The flowing N₂ was then replaced by a N₂ + NO₂ (0.98 ± 0.05) ppm mixture for 3 min. After that, the chamber was flushed with pure N₂. During the whole process the film conductance was measured as a function of the time every 15 s at fixed temperature and voltage (1 V).

All the electrical measurements were performed without light irradiation (dark measurements).

3. Results

Table 1 summarizes the heat treatments with temperature and time for the CuPc samples and the analyses performed on these samples. All the treatments were carried out in air. An abbreviating name has been chosen for every sample to lighten the text. All the GDS samples were investigated by IBA in order to determine the evolution of their composition after heating and, in particular, the possible release of volatile species. For XAS experiment CuPc thin films were also deposited by standard vacuum evaporation (VE) on Kapton films and analyzed before and after treatment at 250 and 290 °C for 14 h, to compare these samples with GDS films.

3.1. Ion Beam Analysis. Table 2 reports the Cu, C, N, and O atomic contents of the as-deposited and heated films as calculated by IBA measurements. As previously observed, copper content of every sample was determined by RBS and carbon, nitrogen, and oxygen contents were measured by NRA. The only exception is the sample 290C14h, whose carbon and oxygen contents were measured by RBS. For this sample the relative error on the carbon and oxygen contents was 10–15% and the resulting error on the C/Cu and O/Cu atomic ratios was about the same. For the same sample nitrogen content was under the detection threshold.

In the sample ASDEP the copper content is 5.5×10^{16} atom/cm². Assuming that every Cu atom belongs to a CuPc

(22) Neville, M.; Livins, P.; Yacoby, Y.; Rehr, J. J.; Stern, E. A. *Phys. Rev. B* **1993**, *43*, 14126.

(23) Neville, M. J. *Synchrotron Radiat.* **2001**, *8*, 322.

(24) Ankudinov, A. L.; Ravel, B.; Rehr, J. J.; Conradson, S. D. *Phys. Rev. B* **1998**, *58*, 7565.

(25) Brown, C. J. *J. Chem. Soc. A* **1968**, *89*, 2488.

(26) *Practical Surface Analysis*, 2nd ed.; Briggs, D., Seah, M. P., Eds.; John Wiley & Sons: Chichester, 1990; Vol. 1.

(27) *Polymer Surface Modification: Relevance to Adhesion*; Mittal, K. L., Ed.; VSP: Utrecht, The Netherlands, 1996.

Table 2. Atomic Composition of CuPc Samples as Measured by Ion Beam Analysis

sample	Cu (10^{16} atom/cm 2) ($\pm 5\%$)	C (10^{16} atom/cm 2) ($\pm 5\%$)	N (10^{16} atom/cm 2) ($\pm 5\%$)	O (10^{16} atom/cm 2) ($\pm 5\%$)	C/Cu ($\pm 10\%$)	N/Cu ($\pm 10\%$)	O/Cu ($\pm 10\%$)
ASDEP	5.5	142	40	6.3	26	7.3	1.15
290C30	5.5	135	40	8.8	24.5	7.3	1.6
290C1h	5.2	102	31	7.3	20	6.0	1.4
290C2h	5.4	76	25	5.4	14	4.6	1.0
290C3h	5.3	55	17	5.3	10	3.2	1.0
290C4h	5.4						
290C14h	5.5	7.7	-	13	1.4	-	2.4
250C14h	5.4	78	25	6.5	14	4.6	1.2

molecule, the film consists of 5.5×10^{16} molecules/cm 2 , which means that the film thickness is about 1.77 μm , assuming a density of 3.1×10^{20} mol/cm 3 .¹⁵

3.2. FT-IR Analysis. FT-IR spectra of the CuPc samples before and after heating at 290 °C show the presence of all the typical features of the CuPc molecule. In the sample ASDEP a peak at 2230 cm $^{-1}$ (C \equiv N group) is found, whose intensity decreases at increasing heating time until it disappears in the sample 290C4h.

To analyze the crystal structure of the heated films, the following regions of the FT-IR spectra have been reported in Figure 1: 1190–1050, 975–840, and 800–700 cm $^{-1}$. In fact, it is well-known that α and β polymorphs of MPCs are characterized by some IR peaks related to the short-range neighbor interactions.^{28–30} As can be seen, the out-of-plane hydrogen bending mode (γ (C–H)) peak, which is centered at 726 cm $^{-1}$ in the sample ASDEP, undergoes a splitting in two components centered at 731 cm $^{-1}$ (β phase) and 722 cm $^{-1}$ (α phase) ever since 30 min. At increasing heating time the two peaks become more resolved and the relative intensity of the peak at 722 cm $^{-1}$ decreases until it becomes a small shoulder of the other peak in the spectrum of the sample 290C14h. A similar behavior is followed by the broad peak centered at 776 cm $^{-1}$: at increasing heating time it splits into two better solved peaks at 780 cm $^{-1}$ (β) and 772 cm $^{-1}$ (α) and then the intensity of the latter peak gradually decreases. In the region from 975 to 840 cm $^{-1}$, the peak centered at 870 cm $^{-1}$ (α), which is not solved from the peak at 877 cm $^{-1}$ (β), decreases at increasing heating time until it disappears in the sample 290C14h. The peak centered at 951 cm $^{-1}$ splits into two components at 949 and 957 cm $^{-1}$ (β). Finally, in the 1190–1050 cm $^{-1}$ region the peak at 1091 cm $^{-1}$ shifts to 1089 cm $^{-1}$ and two shoulders appear at 1100 cm $^{-1}$ (β) and 1174 cm $^{-1}$ (β).

To discriminate the effects of heat treatments on the central copper atom and on the remaining part of the CuPc molecule, the absolute intensities of the peak at 900 cm $^{-1}$ and of the peak at 1121 cm $^{-1}$ together with their ratio have also been measured as a function of heating time and temperature (see Supporting Information). In fact the peak at 900 cm $^{-1}$, which has been ascribed either to the Cu–N vibration³¹ or to C–N= bending,³² is strongly related to the presence of

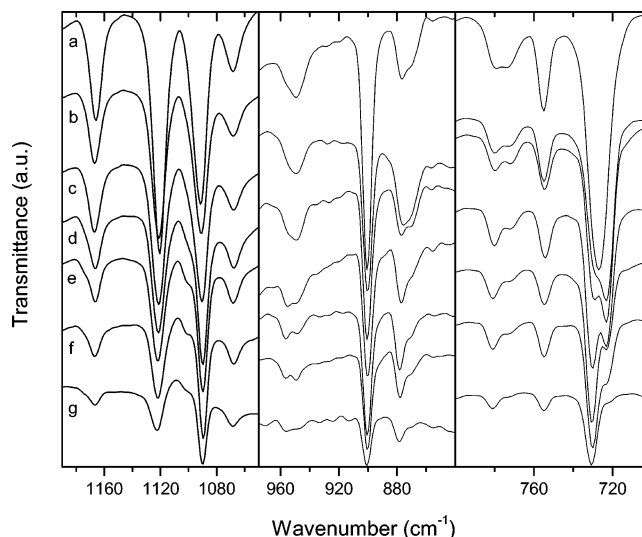


Figure 1. FT-IR spectra of GDS films ASDEP (a) and heated at 290 °C for times ranging from 30 min (b) to 14 h (g). The regions are 1190–1050, 975–840, and 800–700 cm $^{-1}$.

copper atom in the phthalocyanine molecule and its position changes when different metal atoms replace copper in the center of the molecule.²⁵ On the other hand, the peak at 1121 cm $^{-1}$, which corresponds to the in-plane C–H vibration of the phenyl ring,³³ is independent of the copper presence. For this comparison the peak intensity instead of the integral was chosen because the full-width at half-maximum (fwhm) was about the same for all the samples. Although the absolute intensity of both peaks decreases at increasing treatment time and temperature, their ratio remains nearly constant (about 0.3).

3.3. SEM. SEM micrographs of samples before and after heating at 290 °C for different times are displayed in Figure 2. The appearance of needlelike structures on the film surface is already evident in the sample 290C30. At increasing heating time the lateral sizes of the needles increase.

3.4. UV–Vis Absorption Analysis. UV–Vis absorption spectra of the heated samples are displayed in Figure 3. The sample ASDEP exhibits the Q band peaked at 613 and 680 nm and the B band (Soret band) peaked at 211, 262, and 334 nm. At increasing heating time the intensity of both bands decreases. Moreover, a shift of the maximum peaks takes place: the shift is already evident for the B band in the sample 290C30 and for the Q band in the sample 290C2h.

3.5. XAS Analyses. The EXAFS signals of the CuPc samples are reported in Figure 4. In Figure 5a the Fourier

(28) Sidorov, A. N.; Kotlyar, I. P. *Opt. Spectrosc.* **1961**, *11*, 92.

(29) Hassan, A. K.; Gould, R. D. *Phys. Status Solidi A* **1992**, *91*, 132.

(30) Sadaoka, Y.; Goepel, W.; Suhr, B.; Rager, A. *J. Mater. Sci. Lett.* **1990**, *1481*, 9.

(31) Kobayashi, T.; Kurokawa, F.; Uyeda, N.; Suito, E. *Spectrochim. Acta A* **1970**, *26*, 1305.

(32) Achar, B. N.; Lokesh, K. S. *J. Solid State Chem.* **2004**, *177*, 1987.

(33) Shurvell, H. F.; Pinzuti, L. *Can. J. Chem.* **1966**, *44*, 125.

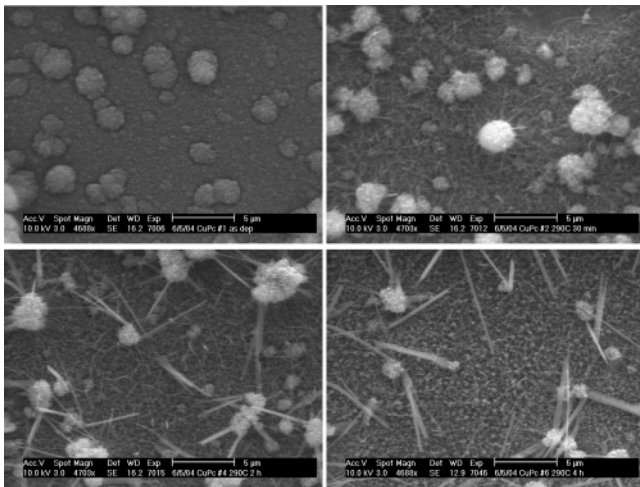


Figure 2. SEM images of GDS films: ASDEP (upper left), 290C30 (upper right), 290C2h (lower left), and 290C4h (lower right).

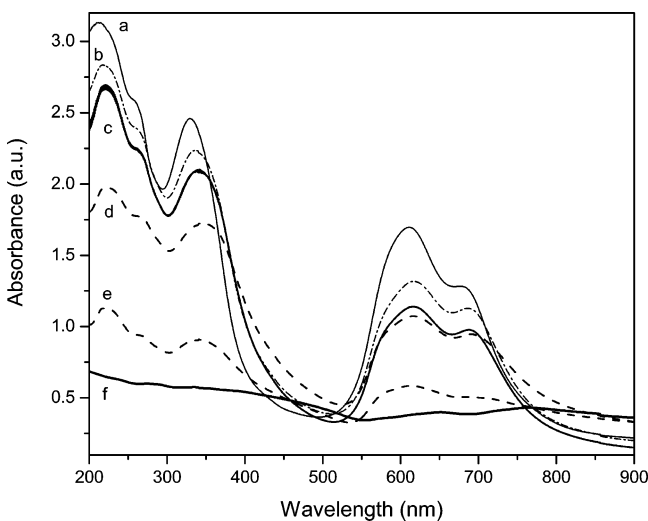


Figure 3. UV-Visible absorption spectra of heated GDS films: (a) ASDEP; (b) 290C30; (c) 290C1h; (d) 290C2h; (e) 290C3h; (f) 290C14h.

transform moduli are shown: in all the cases a main peak is visible at $R \cong 1.7 \text{ \AA}$, which corresponds to the first Cu–N coordination of the CuPc molecule. In Figure 5b the first shell contribution to the whole EXAFS spectrum in the k -space is reported; the first shell fit is superimposed to the experimental data in both R - and k -spaces (Figures 5a and 5b, respectively). The fit results for the first Cu–N shell are reported in Table 3. The results show that heat treatments had no significant effect on the Cu first shell coordination: in all the cases the first shell is composed of 3–4 N atoms at a distance of 1.91–1.94 \AA , which within the experimental uncertainties is in agreement with the local structure around Cu of a CuPc molecule, composed by 4 N atoms at 1.93 \AA .²⁵ A systematic EXAFS study (not reported here) on evaporated CuPc samples heated at different temperatures (EVASDEP, EV250C14h, and EV290C14h) led to the same conclusions.

In Figure 6a the XANES spectra at the Cu K-edge are reported for the samples ASDEP, 250C14h, 290C14h, and EV290C14h. The spectrum of the sample 290C14h looks quite different: in particular, the first peak just on the edge jump ($E \sim 8985 \text{ eV}$) is less pronounced and the peak located just above the photoelectric absorption edge (labeled “A” in

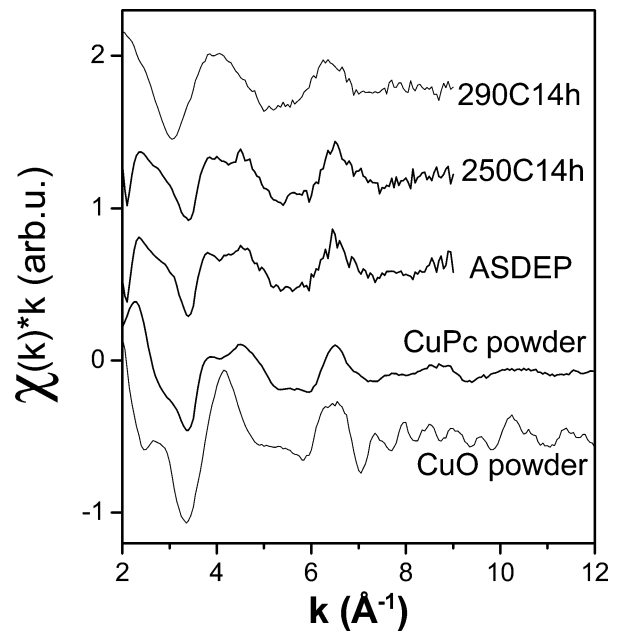


Figure 4. EXAFS data for GDS samples (ASDEP, 250C14h, and 290C14h), CuPc powder, and crystalline CuO (this last one has been measured at liquid nitrogen temperature).

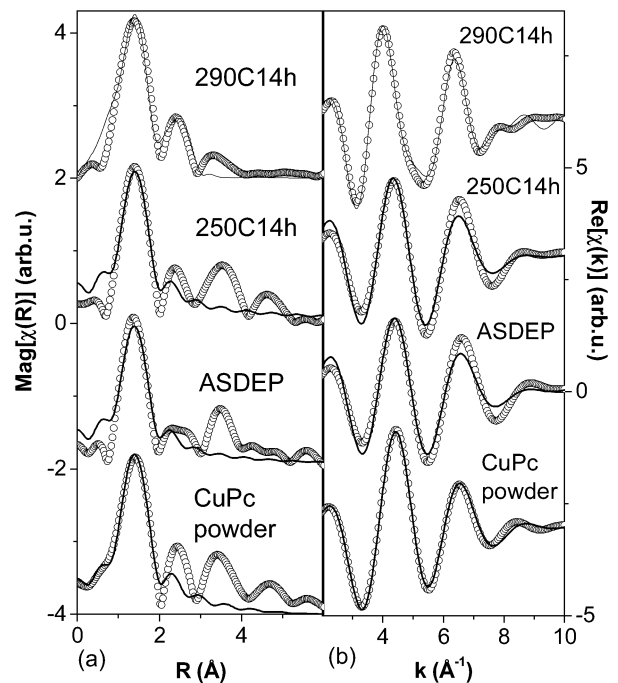


Figure 5. (a) Moduli of Fourier transformed EXAFS spectra (in the range $k = 3\text{--}8 \text{ \AA}^{-1}$, open circles) and first shell fit (solid line). (b) Back-transformed first shell EXAFS data (open circles) and corresponding fit (solid line).

Figure 6a) is narrower for the sample 290C14h than for the other samples (including the CuPc powder one, reported in Figure 6b). It is worth noting that the XANES spectrum recorded for the CuPc solution (see Figure 6b) is almost identical to that of CuPc crystalline powder: this indicates that the main features of the CuPc spectrum are mainly due to the CuPc molecular structure rather than to the packing of the CuPc molecules into the crystal. This assesses that the modifications observed in the XANES spectrum of the sample 290C14h are due to a (partial) structural decomposition of the CuPc molecules. It is found that the spectrum of

Table 3. Results of the EXAFS Analysis of the First Atomic Shell for GDS Samples and CuPc Powder: N Is the Coordination Number of the Nitrogen Shell, R the Cu–N Interatomic Distance, and σ^2 the Debye–Waller Factor^a

sample	N	R (Å)	σ^2 (Å ²)
CuPc powder	4 (fixed)	1.91 ± 0.02	0.002 ± 0.003
ASDEP	3.3 ± 0.7	1.91 ± 0.02	0.002 (fixed)
250C14h	3.6 ± 0.7	1.94 ± 0.02	0.002 (fixed)
290C14h	4 ± 2	1.94 ± 0.04	0.006 ± 0.002
Cu–O (Cu–O coord)	4	1.95	

^a The crystallographic data for the CuO crystal are reported for comparison.

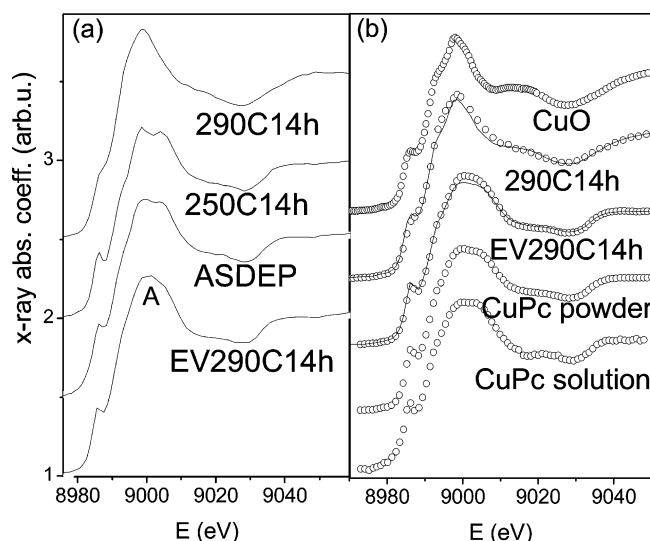


Figure 6. (a) XANES spectra of the samples EV290C14h, ASDEP, 250C14h, and 290C14h. (b) XANES spectra of EV290C14h and 290C14h, superimposed to the corresponding best fit curves obtained as a linear combination of the two CuO and CuPc powder spectra (also reported). The XANES spectrum of the CuPc solution is also shown for comparison.

the sample 290C14h is similar to the spectrum recorded for a CuO crystalline powder. In Figure 6b the two spectra (290C14h and EV290C14h) are compared with those from CuPc and CuO standard compounds. A linear combination fitting performed on the two spectra, using CuO and CuPc powder as basis, is superimposed to the experimental data: the best fitting curve for the spectrum of the sample 290C14h is a linear combination of 75% (CuO)–25% (CuPc powder), indicating that the film was partially decomposed and about 3/4 of the Cu atoms bind themselves to O to form CuO. In contrast, no CuO contribution was found in the sample EV290C14h.

On the basis of these XANES findings, the fitting of the sample 290C14h included also Cu–O and Cu–Cu correlations at 1.98 and 2.93 Å, typical of very disordered or amorphous CuO, as confirmed by the large Debye–Waller factors. The coordination numbers range from 1 to 2 for the Cu–N component and from 2 to 4 for the Cu–O component.

3.6. XPS. The survey and expanded Cu 2p XPS spectra of the as-deposited and thermally treated samples are reported in Figure 7. The survey spectrum of the sample ASDEP shows the C, Cu, O, and N signals. In the spectrum of the sample 290C14h an increase of copper and oxygen signals and a decrease of carbon and nitrogen signals can be observed. Table 4 reports the quantitative compositions of these two surfaces. The Cu 2p expanded region shows two

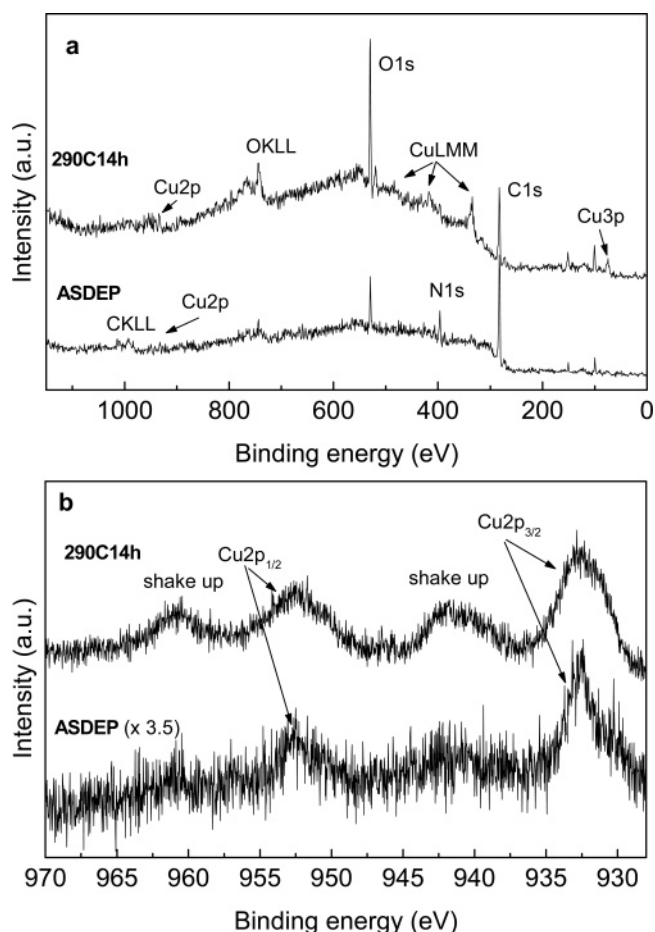


Figure 7. XPS spectra of GDS films ASDEP and 290C14h: (a) survey; (b) Cu 2p expanded region.

Table 4. Atomic Percentages of Carbon, Oxygen, Nitrogen, and Copper of Samples ASDEP and 290C14h, as Measured by XPS

sample	C	O	N	Cu
ASDEP	69.6	14.1	12.2	0.7
290C14h	45.2	35.3	5.3	3.5

main peaks, i.e., Cu 2p_{1/2} and Cu 2p_{3/2} doublet attributed to a two-holes final state 2p⁵3d¹⁰L, where L means a hole in the ligand molecular orbitals. The broad bands associated with the main peaks, i.e., the shake up, are attributed to a two holes final state of 2p⁵3d⁹. Copper in the Cu Pc molecule shows low-intensity shake-up bands thanks to the presence of ligand, which leads to a two holes final state configuration having complete d orbitals (2p⁵3d¹⁰L) similar to Cu(I) species. In the absence of Pc ligand the shake up associated with the d ← d transitions in the d⁹ configuration of the Cu(II) become intense. The composition variation on going from the ASDEP to the 290C14h sample, as well as the increase of the shake-up bands associated with the Cu2p_{1/2} and Cu2p_{3/2} doublet, indicate a partial decomposition of CuPc into byproducts such as oxide-hydroxide and carbonate of Cu(II).

3.7. Surface Electrical Conductance vs Temperature.

Figure 8 shows the trend of the electrical conductance of CuPc films before and after heating as a function of sample temperature in the range from 20 to 170 °C as measured in a nitrogen atmosphere. The samples tested were as follows: ASDEP, 250C14h, 290C30, and 290C3h. The temperature was first increased from room temperature to its maximum

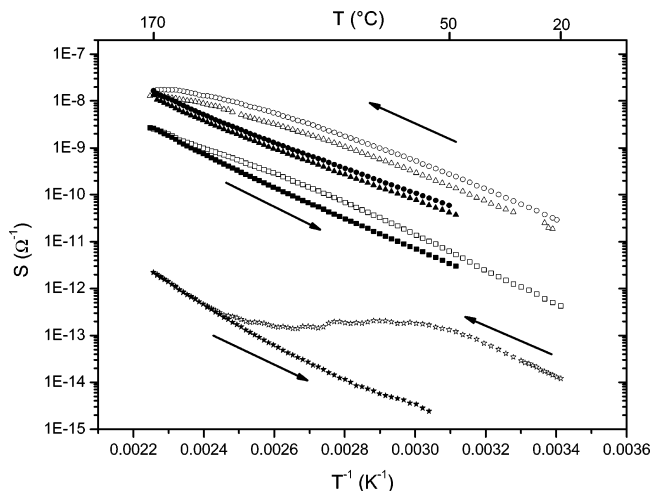


Figure 8. Surface electrical conductance vs reciprocal temperature, at increasing temperature (open symbols) and decreasing temperature (full symbols), of CuPc films ASDEP (star), 250C14h (triangle), 290C30 (circle), and 290C3h (square).

Table 5. Surface Electrical Conductance at 170 °C ($S_{170^{\circ}\text{C}}$) and Activation Energy (E_{act}) of the CuPc Samples

sample	$S_{170^{\circ}\text{C}}$ (Ω^{-1})	E_{act} (eV)
ASDEP	2.2×10^{-12}	0.33
250C14h	1.3×10^{-8}	0.27
290C30	1.6×10^{-8}	0.27
290C3h	2.6×10^{-9}	0.29

value, and then it was allowed to cool. In the case of the sample ASDEP the strong difference between the increasing curve and the decreasing one is due to the effects of oxygen absorption during its short storage period before the measurement: as a matter of fact it is well-known that oxygen molecules absorbed in MPC films increase their conductance.^{34,35} For this reason while the decreasing curve follows an exponential trend, the absorbed oxygen increases the film conductance at the lowest temperatures until it is released ever since the sample reaches the temperature of 60 °C. The same effect was observed in evaporated films,³⁶ but it was ascribed to the desorption of water vapor. The oxygen effect is much less pronounced in the heated films where the difference between the increasing and decreasing curves is small and for the samples 250C14h and 290C3h the curves coincide only at the highest temperature. This suggests that the oxygen release is much lower than for ASDEP film and it takes place during the whole measurement, maybe due to the lower porosity of heated samples. The heated films also exhibit a much higher conductance with respect to the sample ASDEP, as shown in Table 5. However, for all the samples the conductance at 170 °C is about 3 orders of magnitude higher than that at 50 °C.

In Table 5 the activation energy (E_{act}) of the tested samples is also reported. The activation energy was calculated by fitting the decreasing curve assuming a conductance S relationship of the form $S = S_0 \exp(-E_{\text{act}}/kT)$, where S_0 is a constant, k is Boltzmann constant, and T is the sample temperature. The activation energy slightly decreases after heating.

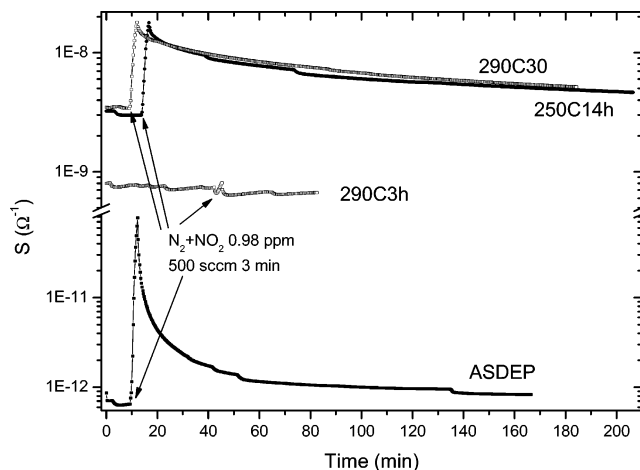


Figure 9. Electrical response to NO_2 of CuPc films ASDEP, 250C14h, 290C30, and 290C3h.

3.8. Electrical Response to NO_2 . The electrical response of CuPc samples upon NO_2 exposure is compared in Figure 9. After the starting sample conditioning in nitrogen flux, the NO_2 -containing mixture was admitted for 3 min and then nitrogen was fluxed once again.

The tested films behave in a very different way: in the case of the sample ASDEP the conductance increase during NO_2 exposure is very pronounced and is about 2 orders of magnitude, while for the samples 250C14h and 290C30 the increase is only 6 times the value before NO_2 admittance. On the other hand, the sample 290C3h is completely insensitive to NO_2 , at least at the concentration used in these measurements: the small change of conductance after NO_2 admittance is thought to be due to transient flow instabilities which are not physically significant. After NO_2 removal, a signal recovery takes place for all the sensitive samples. The recovery is faster for the sample ASDEP than for the heated ones: as a matter of fact, the conductance becomes 1.6 times its pristine value before NO_2 admittance after 1 h and 22 min for the sample ASDEP, after 2 h and 52 min for the 250C14h sample, and after 2 h and 35 min for the 290C30 sample. These data are particularly significant considering that the conductance increase is much higher for the sample ASDEP than for the other samples. At the end of the measurement the conductance of this sample was 1.3 times its pristine value.

4. Discussion

Previous measurements of the chemical composition of CuPc films deposited by GDS technique showed that the incorporation of molecular fragments in the film increases at increasing deposition time: in particular, a sample deposited for 175 s mainly consisted of integer CuPc molecules as shown by ion beam analysis and FT-IR,¹⁵ while several-minutes-long depositions gave rise to films containing a significant fraction of damaged molecules. In this work the ASDEP film has been deposited for a short time (150 s) so that a stoichiometric composition should be expected. Notwithstanding this, ion beam analysis of this sample shows that the C/Cu and N/Cu atomic ratios are slightly lower than the expected ones for a CuPc molecule, that is, 32 and 8,

(34) Dahlberg, S. C.; Musser, M. E. *J. Chem. Phys.* **1980**, *72*, 6706.

(35) van Faassen, E.; Kerp, H. *Sens. Actuators B* **2003**, *88*, 329.

(36) Shihub, S. I.; Gould, R. D. *Thin Solid Films* **1996**, *290–291*, 390.

respectively (Table 2). However, it must be observed that this “understoichiometry” is relatively low: in fact, in the case of nitrogen, the expected ratio is inside the uncertainty range of the experimental data; in the case of carbon, the difference is about 10%. This means that the film contains only a small fraction of molecular fragments, as confirmed by FT-IR and UV–visible spectra of sample ASDEP (see Supporting Information and Figure 3, respectively), which show almost exclusively the typical CuPc features. These data indicate that the predominant species in the deposited film is then undamaged copper phthalocyanine. Part of the incorporated fragments gives rise to the small peak at 2230 cm^{-1} ($\text{C}\equiv\text{N}$ group) in the FT-IR spectrum of the film ASDEP (see Supporting Information): this peak was also found in GDS films deposited for longer times (4–20 min).¹⁵ The appearance of the same peak was observed in the case of CuPc sublimated in argon atmosphere as well and was ascribed to the presence of CuPc fragments such as phthalodinitrile.³⁷ The incorporation of molecular fragments in the film ASDEP is only partially unexpected, taking into account the very irregular trend of the CuPc deposition rate as compared to other organic compounds:¹⁵ as a matter of fact, the lower the deposition rate, the lower the sublimation rate of CuPc molecules, so that both sputtering of the damaged molecules on the target surface and sublimation of low-boiling molecular fragments become important and give rise to the emission of low-weight compounds which can be easily incorporated in the film. As far as the microstructure of the sample ASDEP is concerned, FT-IR and UV–Vis spectra (Figures 1 and 3) confirm that it consists of a mixture of α and β CuPc polymorphs as previously found.¹⁵

Chemical composition, microstructure, and morphology undergo significant changes during heat treatments. While copper content does not change after heating at 250 and 290 °C for all the treatment times, the atomic contents of carbon and nitrogen drastically decrease ever since the treatment at 250 °C, where they become 0.55 and 0.62 the pristine values, respectively (Table 2). At 290 °C the carbon and nitrogen losses increase with the heating time: after 14 h the carbon content is only 0.05 the pristine value. XPS analysis confirms the pronounced decrease of C/Cu and N/Cu atomic ratios in the sample heated at 290 °C for 14 h, while a much lower decrease of O/Cu and a strong increase of O/C and O/N are found as well. In agreement with the decrease of the nitrogen and carbon contents, a decrease of some IR peaks of CuPc is also observed: in particular, the absolute intensity of the peaks of Cu–N (900 cm^{-1}) and C–H (1121 cm^{-1}) decreases at increasing heating temperature and time and it becomes about 0.2 times the pristine value in the sample 290C14h (see Supporting Information). Taking into account that copper content does not change in the heated samples, this indicates that Cu–N bond is broken and copper remains in the film while nitrogen is released together with part of the CuPc molecule, as confirmed by the almost constant value of the ratio between the intensity of the Cu–N peak and that of the C–H peak in the heated samples (see Supporting Information). This means that the main effect of the heat

treatment is not the sublimation of CuPc molecules, but the gradual molecular decomposition with the consequent formation of volatile and nonvolatile fragments. The release of volatile fragments is confirmed by the gradual disappearance of the $\text{C}\equiv\text{N}$ peak in the FT-IR spectra of the heated samples. The decomposition of CuPc molecules gives rise to the gradual decrease of both Q and B bands of CuPc in the UV–Vis absorption spectra of the heated samples (Figure 3).

As to the microstructure of the heated films, the aggregates of residual CuPc molecules undergo structural changes as a function of heating time as highlighted by FT-IR and UV–Vis analyses and SEM images (Figures 1, 2, and 3). In particular, in the samples heated at 290 °C, a structural rearrangement occurs ever since 30 min, as shown by the enhanced separation of the overlapping $\gamma(\text{C–H})$ peaks of α and β polymorphs. At increasing heating time the IR features of the α phase progressively disappear and only the peaks of the β polymorph remain in the sample 290C14h. The disappearance of the α phase is also confirmed by the shift of the Q and B bands to higher wavelengths in the UV–Vis absorption spectra of the heated samples. Moreover, the needlelike β crystallites³⁸ shown by SEM become the prevailing structures on the film surface at increasing heating time.

On one hand, the structural changes observed in the heated samples could be foreseen on the basis of the similar behavior of evaporated films; on the other hand, the decomposition of CuPc molecules is partially unexpected, taking into account the particularly high thermal stability of copper phthalocyanine. As a matter of fact, TGA and DTA analyses of CuPc powder in air show that the weight loss becomes significant starting from temperatures higher than 400 °C; moreover, only at 600 °C CuPc is almost completely decomposed and oxidized and gives rise to the formation of CuO, which becomes the only residual species after heating at 800 °C.³⁷ In the case of the evaporated CuPc films, it should be pointed out that most authors give no particular relevance to a possible weight loss after heating at temperatures lower than 350 °C since the attention is mainly focused on the CuPc phase transformation. For this reason heat treatments are performed in nitrogen atmosphere^{36,38} or in a vacuum^{27,39} to prevent the effects of air or else these effects are neglected.^{11,40,41} To support this belief, it must be noted that evaporated films used in these work did not undergo significant changes after heating at 250 and 290 °C in air and the decomposition of CuPc molecules with the consequent formation of CuO was not detected by XAS measurements. Moreover, thermogravimetric analyses of evaporated CuPc films showed that the 5 wt % weight loss occurred at temperatures of 416 and 423 °C in dry and humid air, respectively.⁴² However, Prabakaran et al.⁴³ showed that

(37) Markova, I. Y.; Kiryukhin, I. A.; Shaulov, Y. K.; Benderskii, V. A.; Grigorovich, S. M. *Russ. J. Inorg. Chem.* **1976**, *21*, 356.

(38) Berger, O.; Fischer, W.-J.; Adolphi, B.; Tierbach, S.; Melev, V.; Schreiber, J. *J. Mater. Sci.: Mater. Electron.* **2000**, *331*, 11.

(39) Dogo, S.; Germain, J. P.; Maleysson, C.; Pauly, A. *Thin Solid Films* **1992**, *219*, 244.

(40) E, J.; Kim, S.; Lim, E.; Lee, K.; Cha, D.; Friedman, B. *Appl. Surf. Sci.* **2003**, *205*, 274.

(41) Zhivkov, I.; Spassova, E.; Danev, G.; Andreev, S.; Ivanov, T. *Vacuum* **1998**, *51*, 189.

(42) Sadaoka, Y.; Sakai, Y.; Jones, T. A.; Goepel, W. *J. Mater. Sci.* **1990**, *25*, 3024.

evaporated films heated at 320 °C for 14 h underwent a thickness decrease from 440 to 200 nm. For the same films heated at 520 °C for 14 h the thickness decreased down to 70 nm and XRD analysis detected the typical peaks of monocline CuO (ICDD 410254), while CuPc completely disappeared. According to the authors, the CuPc molecules decomposed, leaving copper, which was oxidized in air and gave rise to CuO nanoclusters. Moreover, in the case of evaporated films heated at 300 °C for several hours, Hassan and Gould²⁹ observed also a film sublimation, which left only a film shadow on the substrate.

As to the heated GDS samples, the carbon and nitrogen loss indicates that the bond between part of the copper atoms and the phthalocyanine molecules is broken and that volatile fragments are emitted from the films. Taking into account the results of Markova et al.³⁷ and Prabakaran et al.,⁴³ the remaining copper atoms are thought to bind themselves to oxygen atoms to form CuO. This fact is confirmed by XANES and XPS data reported above. The release of volatile species and the consequent formation of CuO take place ever since the treatment at 250 °C so that all the heated films consist of both CuPc molecules and CuO. The presence of CuPc molecules is still evident in the film 290C14h, as shown by FT-IR and XRD analyses.¹⁵ It should also be pointed out that the presence of CuO in the samples 250C14h and 290C14h was not revealed by FT-IR, XRD, and UV–Vis analyses previously performed.¹⁵ This can be explained by taking into account that (i) the typical IR features of CuO as drawn from literature⁴⁴ are very weak and cannot be solved by the CuPc peaks, (ii) the results of Prabakaran et al.,⁴³ which did not find CuO peaks in the XRD spectra of evaporated films heated at 320 °C for 14 h, suggested that the CuPc decomposition should not take place at 290 °C, (iii) the likely presence of a very disordered or amorphous structure of CuO aggregates, as suggested by the XANES results, can prevent the appearance of CuO peaks in the XRD spectra of GDS films, and (iv) the CuO formation is suggested by XANES spectroscopy in the sample 290C14h but not in the 250C14h one.

The CuO formation allows explanation of the electrical behavior of the heated samples. Figure 8 and Table 5 highlight that heating gives rise to an increase of the electrical conductivity of the CuPc film. The increase is visible ever since 30 min at 290 °C. The electrical conductivities of the samples 250C14h and 290C30 are very similar, while a slightly lower value is exhibited by the sample 290C3h. This behavior is in contrast with that of the evaporated films, which undergo a decrease of conductivity when heated at 300 °C for times ranging from 2 to 6 h.^{45,11} Moreover, the decomposition of part of the CuPc molecules should give rise to a decrease of the number of electrical carriers and then to a conductivity decrease. The increase of conductivity cannot be either explained by an α to β phase transition since α and β polymorphs have the same conductivity, according

to Harrison and Ludewig.⁴⁶ On the other hand, CuO has a lower electrical resistivity with respect to CuPc: as a matter of fact, the resistivity at room temperature of CuO in the melaconite form⁴⁷ is $6.0 \times 10^5 \Omega \text{ cm}$ against $10^{10}\text{--}10^{11} \Omega \text{ cm}$ of the pure single-crystal CuPc⁴⁸ so that the replacement of CuPc by CuO should give rise to the observed conductivity increase in the heated films. The formation of CuO is also in agreement with the slight decrease of the activation energy in the heated samples (Table 5) since E_{act} of CuO is lower than that of CuPc (0.15 eV for CuO⁴⁹ against 0.65 eV,⁴⁶ 0.82 eV,⁴² 1.5 eV,⁵⁰ 0.30 eV (α CuPc), and 0.78 eV (β CuPc)⁵¹).

As to the electrical response to NO₂, the main effect of heating is a reduction of the response speed and an increase of the recovery time. Moreover, for the sample 290C3h the film response is drastically reduced. The sensing behavior of the heated GDS films is once more different from that of evaporated films, which showed an improvement of response and recovery rates after heating at 300 °C for 4 h without a significant decrease of the film response.⁴⁵ The different behavior of GDS films can be explained by taking into account several contributions: (i) The decomposition of CuPc molecules determines a decrease of the number of molecules which can interact with NO₂ so that the resulting change of electrical current will be lower. (ii) The replacement of CuPc by CuO determines a decrease of the whole film sensitivity because CuO is not sensitive to NO₂. (iii) At the beginning of the exposure to NO₂, the interaction between CuPc and NO₂ takes place mainly on the surface of the CuPc molecular aggregates, which can be even located in depth, taking into account the particularly high porosity of GDS films. However, these places are also the preferential sites for the interaction between CuPc and oxygen/water vapor during the heating treatments, where the CuPc decomposition and the formation of CuO first take place. For this reason CuO can be a hindrance to NO₂ molecules to reach the CuPc molecules and the increase of the measured current becomes slower. (iv) The NO₂ diffusion into the heated films is further hindered by the gradual disappearance of α phase domains since packing density of this phase is lower than that of β phase. The CuO hindrance to NO₂ diffusion and the disappearance of α phase also account for the much longer recovery times of heated films as compared to the sample ASDEP.

To sum up, the very different effects of heat treatments on GDS films as compared to the evaporated ones are thought to be mainly due to their much higher porosity which allows a larger number of CuPc molecules to interact with the atmosphere, giving rise to the CuPc decomposition and to the CuO formation. Moreover, the presence of molecular

(43) Prabakaran, R.; Kesavamoorthy, R.; Reddy, G. L. N.; Xavier, F. P. *Phys. Status Solidi B* **2002**, *229*, 1175.

(44) SDBSWeb: <http://www.aist.go.jp/RIODB/SDBS/>, National Institute of Advanced Industrial Science and Technology, Dec 06, 2005.

(45) Sadaoka, Y.; Jones, T. A.; Revell, G. S.; Goepel, W. *J. Mater. Sci.* **1990**, *25*, 5257.

(46) Harrison, S. E.; Ludewig, K. H. *J. Chem. Phys.* **1966**, *45*, 343.

(47) Berger, L. J.; Pamplin, B. R. *CRC Handbook of Chemistry and Physics*, 84th ed.; Lide, D. R., Ed.; CRC Press: Boca Raton, FL, 2003; pp 12–106.

(48) Park, C.; Yun, D.H.; Kim, S. T.; Park, Y. W. *Sens. Actuators B* **1996**, *30*, 23.

(49) Serin, N.; Serin, T.; Horzum, S.; Celik, Y. *Semicond. Sci. Technol.* **2005**, *20*, 398.

(50) Ambily, S.; Menon, C. S. *Solid State Commun.* **1995**, *94*, 485.

(51) Moser, F. H.; Thomas, A. L. *The Phthalocyanines, Vol. I: Properties*; CRC Press: Boca Raton, FL, 1983; p 177.

fragments, which can easily sublime, and of amorphous CuPc domains, which have a low thermal stability, decreases the cohesive forces between the CuPc molecules and between the molecular aggregates so that they can be easily reached and decomposed by the gaseous species. The effects of the deep penetration of gaseous species in GDS films were already well highlighted in a previous study on the changes of the IR features of these films due to NO₂ absorption.⁵² On the other hand, in the case of the evaporated films the interaction is thought to take place mostly on the film surface and the film compactness strongly hinders the diffusion of oxygen and water vapor into the film. Therefore, after an initial decomposition of the first molecular layers, the gaseous species are hindered from further diffusion and interaction with CuPc molecules. Only at higher temperatures the gaseous species can diffuse into the evaporated films and give rise to a pronounced CuPc decomposition, as shown by the results of Prabakaran *et al.*⁴³ The barrier effect of the first oxidized molecular layers can also explain the persistent aggregates of residual CuPc molecules in the sample 290C14h.

A final remark must be made on the possible effects of the presence of molecular fragments in the deposited films on the evolution of the film properties during heat treatments, which is the main theme of this work. Besides the cited effects on the cohesive forces between the CuPc molecules, the molecular fragments are not deemed to affect considerably the evolution of the film properties during heat treatments: as a matter of fact, the evolution of structure, morphology, and optical absorption is exactly the same in the case of stoichiometric samples as shown in a previous work.⁵ As to the film composition, the presence of fragments can slightly affect the C/Cu and N/Cu atomic ratios of the single heated samples but it does not modify the decreasing trend of these ratios, which is the most important outcome of IBA data. The evolution of the surface electrical conductance is strongly related to the evolution of the film composition and especially to the formation of CuO as well as the evolution of the electrical response to NO₂ is particularly related to the decomposition of CuPc molecules. Moreover, the effects of the incorporated fragments become even smaller at increasing treatment time since the volatile fragments are gradually released by the film as shown by the decrease of the peak at 2230 cm⁻¹ (C≡N peak) in the IR spectra of the samples heated at 290 °C until its complete disappearance in the sample 290C4h.

5. Conclusions

The effects of heat treatments on the properties of copper phthalocyanine films deposited by glow-discharge-induced sublimation have been investigated by using several analyti-

cal techniques. The CuPc samples have been heated in air at 250 °C for 14 h and at 290 °C for times ranging from 30 min to 14 h.

Drastic changes of the elemental composition of the heated films have been revealed by IBA and XPS measurements, which showed a strong decrease of carbon and nitrogen contents against a constant copper amount and an increase of oxygen percentage. The structure of the heated films evolves from the mixture of both α and β phases to the only β phase in the sample treated at 290 °C for 14 h, as shown by FT-IR and UV-vis absorption analysis. SEM images point out the formation of needlelike β crystallites ever since 30 min at 290 °C. The changes of composition, structure, and morphology are related to the treatment temperature and time; that is, the higher the temperature or the time, the more pronounced the changes.

EXAFS measurements show that heat treatments have no effect on the copper first shell, which consists of 3–4 atoms at a distance of 1.91–1.94 Å, that correspond to the local structure of copper in a CuPc molecule, within the experimental uncertainties. On the other hand, XANES and XPS measurements point out the structural decomposition of part of the CuPc molecules which are replaced by copper oxide aggregates: this means that the bond between copper and phthalocyanine is broken and the organic moiety is released while copper binds itself to atmospheric oxygen to give rise to copper oxide. This process takes place ever since the treatment at 250 °C and it is due to the much more porous structure of the GDS films as compared to the evaporated ones, which do not decompose until temperatures higher than 300 °C.

The results of this study give also an important indication on the choice of the working parameters of these films as electrical gas sensing materials: in fact, it has been shown that the response to NO₂ is strongly modified by heat treatments and is dramatically compromised after the treatment at 290 °C for 3 h. Therefore, to ensure a reasonable lifetime to a sensor based on these films, its working temperature should be chosen as a compromise between a high response and reversibility (at temperatures equal to or higher than 150 °C) and a long lifetime (for temperatures lower than 200 °C).

Acknowledgment. This research was financially supported by the Fifth Commission of Istituto Nazionale di Fisica Nucleare (DEGIMON project).

Supporting Information Available: FT-IR spectrum of the sample ASDEP; table containing the absolute intensity of the IR peaks at 900 cm⁻¹ (*I*₉₀₀) and 1121 cm⁻¹ (*I*₁₁₂₁) and their ratio for all the CuPc samples. This material is available free of charge via the Internet at <http://pubs.acs.org>.

CM060303D

(52) Maggioni, G.; Quaranta, A.; Carturan, S.; Patelli, A.; Tonezzer, M.; Ceccato, R.; Della Mea, G. *Surf. Coat. Technol.* **2005**, *200*, 476.